Chaojun CHEN, Shutong CHEN, Yun MA, Junxi ZHU, Chenxi ZHAO, Quanlin GUO, Dezhi GOU, 2026. Design and hardware implementation of bio-inspired neural synchronization anti-interference circuits. *ENGINEERING Information Technology & Electronic Engineering*, 27(7):260117. https://doi.org/10.1631/ENG.ITEE.2026.0117

Design and hardware implementation of bio-inspired neural synchronization anti-interference circuits

Key words: Bio-inspired anti-interference; Neural synchronous dynamics; HH/IZH network models; Hardware implementation

Corresponding author: Dezhi GOU
E-mail: gdz_scu@163.com
ORCID: https://orcid.org/0000-0002-4959-217X

Motivation

- Targeting the limited adaptability and robustness of conventional circuits under strong time-varying disturbances, as well as the lack of a unified framework linking neural synchronization, network topology, and hardware implementation, this study investigates Hodgkin–Huxley (HH) and Izhikevich (IZH) neural networks with different topological structures. By evaluating synchronization stability, energy deviation, disturbance tolerance, and field-programmable gate array (FPGA) resource consumption, a bio-inspired anti-interference circuit framework is developed to achieve stable rhythmic responses and reliable operation under external interference.

Main idea

- A bio-inspired anti-interference circuit framework based on neural synchronization is proposed, which integrates neuron models, network topologies, synchronization stability, and hardware implementation into a unified evaluation system.
- HH and IZH neural networks with different topological structures are constructed and compared, which reveals the effects of coupling strength and topology on synchronization retention, energy deviation, and disturbance tolerance.
- An FPGA-based hardware implementation is developed, which verifies that both HH and IZH circuits can maintain rhythmic firing and waveform integrity under external interference, while the IZH network achieves lower hardware resource consumption.

Method

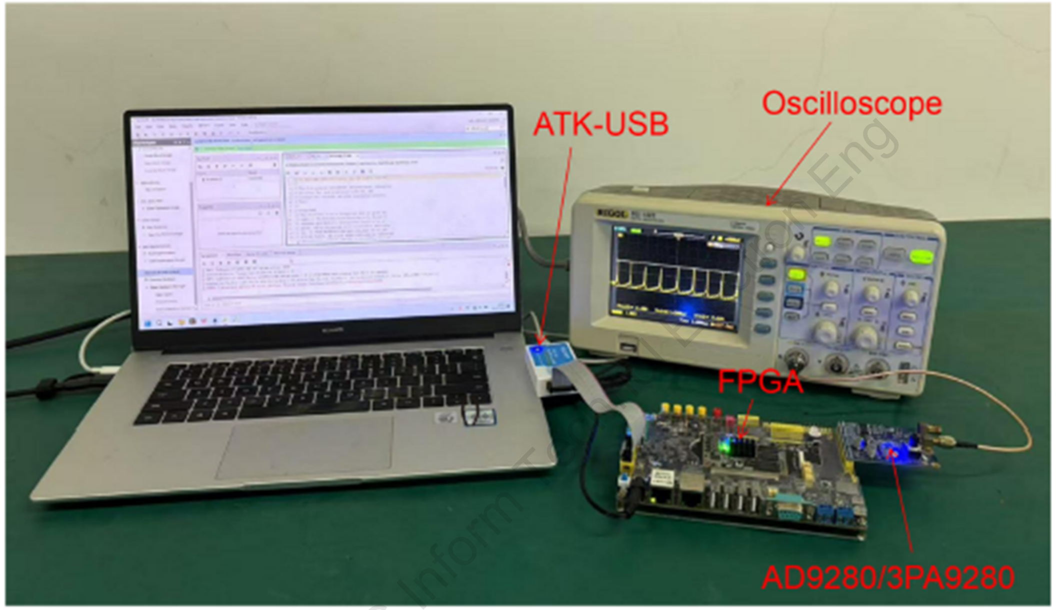

Hardware experimental system diagram

HH Neuron Dynamics

$$C\frac{\mathrm{d}V_i}{\mathrm{d}t} = G_{\mathrm{Na}}m_i^3h_i\left(E_{\mathrm{Na}}-V_i\right)+G_{\mathrm{K}}n_i^4\left(E_{\mathrm{K}}-V_i\right)+G_{\mathrm{L}}\left(E_{\mathrm{L}}-V_i\right)$$

$$+I_{\mathrm{syn}(i,j)}+I_{\mathrm{ext},i}\,,$$

$$\frac{\mathrm{d}m}{\mathrm{d}t}=\alpha_m(1-m)-\beta_m m,$$

$$\frac{\mathrm{d}h}{\mathrm{d}t}=\alpha_h(1-h)-\beta_h h,$$

$$\frac{\mathrm{d}n}{\mathrm{d}t}=\alpha_n(1-n)-\beta_n n,$$

Chemical Synaptic Coupling

$$I_{\mathrm{syn}(i,j)}=I_{\mathrm{syn}(\mathrm{Leonid})}\,,$$

$$I_{\mathrm{syn}(\mathrm{Leonid})}=-C_{\mathrm{m}}S_j\frac{\partial\left(V_i-V_j\right)}{\partial t}+G_{\mathrm{s}}\left(V_{\mathrm{p}}-E_{\mathrm{s}}+V_i-V_j\right).$$

Method

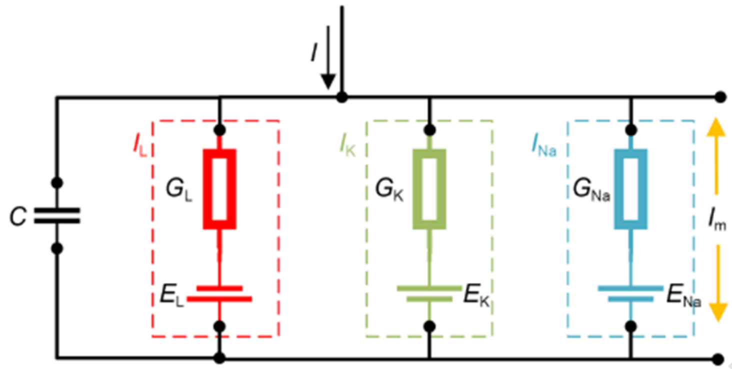

Fig. 1 Action potential of the HH model. I_L, I_K, and I_{Na} denote the leakage, potassium, and sodium ionic currents, respectively. E_L, E_K, and E_{Na} represent the corresponding reversal potentials, while I_m denotes the total ionic membrane current, given by $I_m=I_L+I_K+I_{Na}$

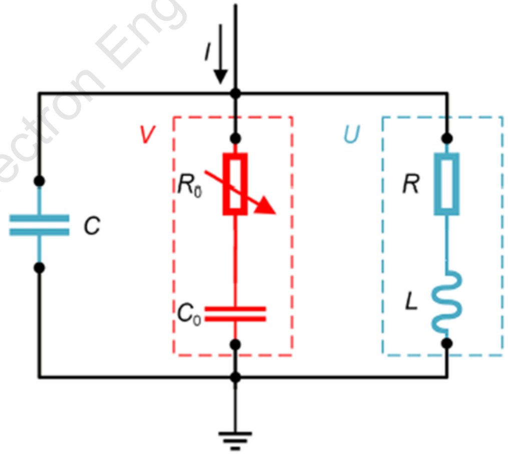

Fig. 2 Action potential of the IZH model. I denotes the external input current injected into the neuron circuit. R_0 denotes the nonlinear voltage-controlled resistance, and C_0 denotes the equivalent capacitance in the membrane-potential branch, which together reproduce the fast nonlinear dynamics of the membrane potential V. R and L denote the resistance and inductance in the recovery-variable branch, respectively, and determine the damping and dynamic response of the recovery variable U

Results

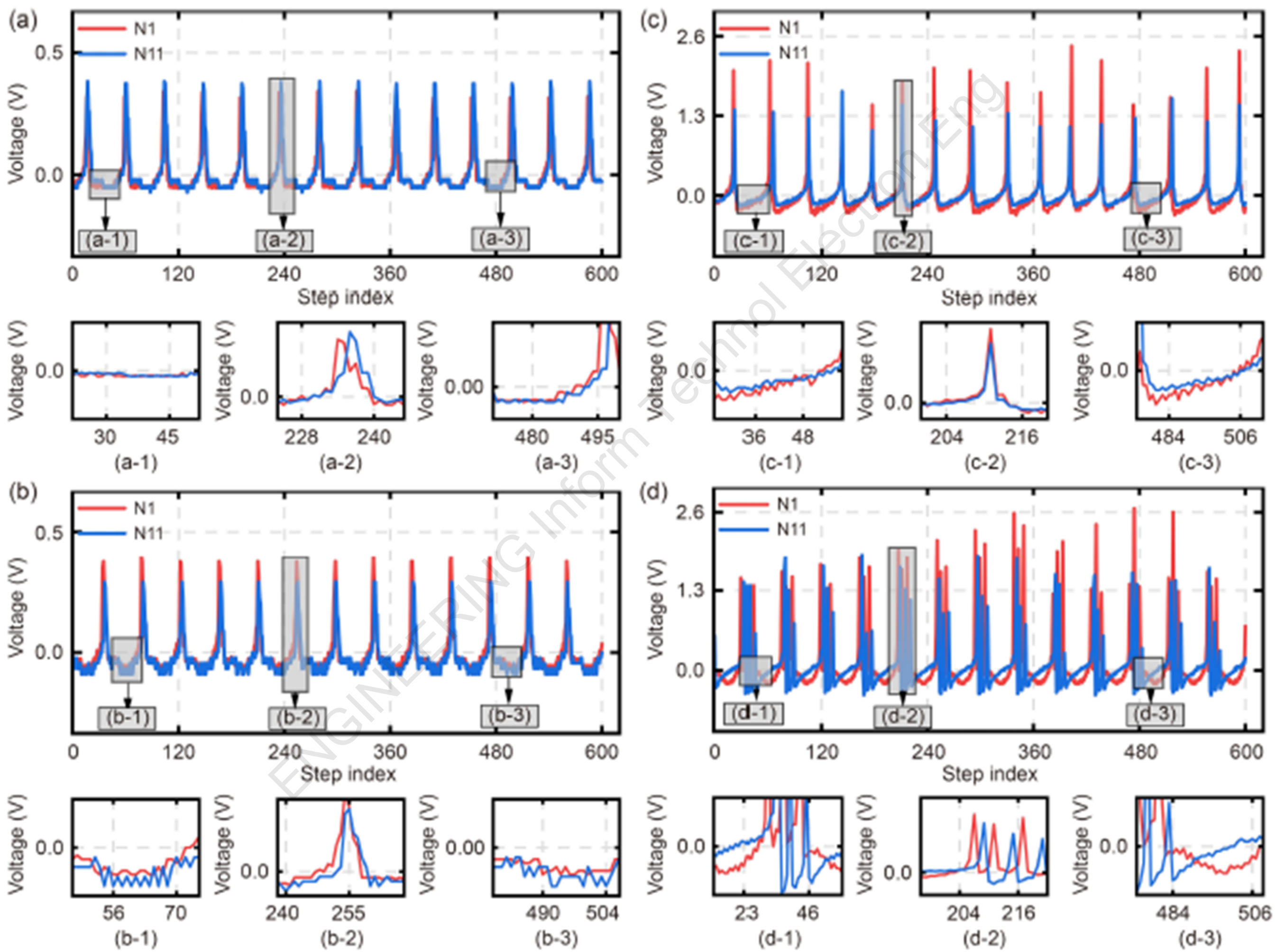

Fig. 10 Action potential diagrams of synchronous states of chain- and ring-type HH and IZH model network circuits: (a) chain-type HH model; (b) ring-type HH model; (c) chain-type IZH model; (d) ring-type IZH model. The enlarged subplots marked as (-1), (-2), and (-3) show three characteristic phases of the action potential, namely, depolarization, repolarization, and hyperpolarization, respectively

Results

Table 3 Synchronization index and reliability indicator of the model before and after being subjected to interference

Model	Synchronization index	Reliability indicator
Chain-shaped, without interference (HH)	0.242 09	0.989 12
Ring-shaped, without interference (HH)	0.516 40	0.989 77
Chain-shaped, without interference (IZH)	0.087 67	0.810 99
Ring-shaped, without interference (IZH)	0.508 48	0.831 51
Chain-shaped, with interference (HH)	0.195 91	0.870 41
Ring-shaped, with interference (HH)	0.148 88	0.836 18
Chain-shaped, with interference (IZH)	0.396 36	0.716 15
Ring-shaped, with interference (IZH)	0.664 82	0.600 67

Conclusions

In this work, we propose a neural synchronization-based bio-inspired anti-interference circuit framework to improve circuit robustness under external disturbances. HH and IZH networks with different topologies are compared in terms of synchronization stability, energy deviation, and disturbance tolerance. FPGA experiments confirm that both circuits maintain rhythmic firing and waveform integrity under interference, while the IZH network requires fewer hardware resources. These results provide a practical reference for adaptive anti-interference circuit design.

Chaojun CHEN received his BE degree in aircraft control and information engineering from China West Normal University in 2024. He is currently pursuing an MS degree in communication engineering at China West Normal University. His current research interests are the design and development of RF integrated circuits and electromagnetic protection bionics.

Dezhi GOU received his PhD degree in radio physics from the College of Electronics and Information Engineering, Sichuan University, China, in September 2022, and is currently a full-time faculty member in the School of Electronic Information Engineering, China West Normal University. He is mainly engaged in the research of electromagnetic field theory, microwave chemistry, and biological effects of electromagnetic radiation.